Journal of Nuclear Materials 390–391 (2009) 830–834

Contents lists available at ScienceDirect

Journal of Nuclear Materials

journal homepage: www.elsevier.com/locate/jnucmat

Plasma radiation distribution and radiation loads onto the vessel during transient events in JET

A. Huber [a,b,*], R.A. Pitts [a,c], A. Loarte [a,d], V. Philipps [a,b], P. Andrew [a,e], S. Brezinsek [a,b], J.P. Coad [a,e], T. Eich [a,f], J.C. Fuchs [a,f], W. Fundamenski [a,e], S. Jachmich [a,g], G.F. Matthews [a,e], K. McCormick [a,f], Ph. Mertens [a,b], J. Rapp [a,h,b], G. Sergienko [a,b], M.F. Stamp [a,e], JET EFDA contributors [1]

[a] JET-EFDA, Culham Science Centre, OX14 3DB, Abingdon, UK
[b] Institut für Energieforschung-Plasmaphysik, Forschungszentrum Jülich GmbH, EURATOM Association, Trilateral Euregio Cluster, D-52425 Jülich, Germany
[c] CRPP, Association EURATOM-Confederation Suisse, EPFL, CH-1015 Lausanne, Switzerland
[d] EFDA Close Support Unit – Garching, Boltzmannstrasse 2, D-85748 Garching, Germany
[e] Euratom/UKAEA Fusion Association, Culham Science Centre, Abingdon, Oxon OX14 3DB, UK
[f] Max-Planck-Institut für Plasmaphysik, EURATOM Association, D-85748 Garching, Germany
[g] Laboratory for Plasmaphysics, ERM/KMS, Association EURATOM-Belgian State, B-1000 Brussels, Belgium
[h] FOM-Instituut Rijnhuizen, Euratom Association, TEC, Nieuwegein, The Netherlands

ARTICLE INFO

PACS:
52.40.Hf
52.25.Vy
52.55.Fa
52.55.Rk

ABSTRACT

The JET bolometer camera system allows greatly improved tomographic reconstruction of the radiation pattern on a timescale of the order of the typical duration of a Type I ELM period (≈0.1–0.4 ms). The ELM-induced radiation is always higher at the inner than at the outer divertor with an approximately linear increase of the asymmetry up to a total ΔW_{ELM} of about 0.6 MJ and a decrease for higher ΔW_{ELM}. Large Type I ELMs with energy losses above 0.65–0.7 MJ show enhanced radiation losses, which are associated with the ablation of thick co-deposited layers in the inner divertor. During the 'compound' phase, plasma contamination can increase but does not usually lead to radiative collapse of the plasma. It is found that the radiation distribution during the transient events is poloidally asymmetric with a maximum of the observed 'radiation peaking factor' for the disruptive current quench and for MARFEs of about 4.5, and less than 5 during VDEs.

1. Introduction

The Type I ELMy H-mode regime is the baseline scenario for operation of ITER in high fusion gain regimes ($Q_{DT} \geqslant 10$) with plasmas of high density ($\langle n_e \rangle \geqslant 10^{20}\,m^{-3}$) and with high plasma energy (~350 MJ) [1]. The major drawback of this operating regime is the ELM-associated periodic power loading of plasma-facing components which can lead to high target erosion and a significant reduction of component lifetimes. In present tokamaks, the plasma energy drop normalised to the pedestal energy $\Delta W_{ELM}/W_{ped}$ is typically 3–10% during a Type I ELM. A significant part of this energy can be found in form of plasma radiation, located mostly in the divertor region (in the present contribution, it is integrated over ~2 ms, which is considerably longer than the ELM-target power deposition of several 100 μs). Systematic studies of the distribution and magnitude of this radiation are required in order to understand and predict the energy deposition by ELMs on plasma-facing components in larger devices such as ITER, where even the smallest Type I ELMs will considerably exceed the maximum energies currently accessible in JET.

2. Experimental set-up

Dedicated experiments aiming at the characterisation of transient loads during large Type I ELMs have been performed during the 2007 JET campaigns at high plasma current and input power: $I_p = 3.0$ MA, $B_T = 3.0$ T, $q_{95} = 3.1$, $\delta_u \sim 0.22$, $\delta_l \sim 0.28$, $\kappa = 1.72$, 19 MW NBI and 1.4 MW ICRH power. The D_2 gas fuelling into the inner divertor scrape-off layer has been progressively decreased from a fuelling rate of $\Gamma_{gas} = 10^{22}$ molecules/s to $\Gamma_{gas} = 0$ to produce a scan in ELM amplitude and frequency at high W_{plasma} (~8 MJ). The JET bolometer camera system has recently been substantially upgraded, allowing significantly improved spatial and temporal resolution of the radiation distribution ($\Delta r \sim 8$ cm in the divertor region, $\Delta t \sim 1$ ms), particularly in the divertor region

* Corresponding author. Address: Institut für Energieforschung-Plasmaphysik, Forschungszentrum Jülich GmbH, EURATOM Association, Trilateral Euregio Cluster, D-52425 Jülich, Germany.
E-mail address: a.huber@fz-juelich.de (A. Huber).
URL: http://www.fz-juelich.de/ief/ief-4 (A. Huber).

[1] See the Appendix of M.L. Watkins et al., Fusion Energy 2006 (Proc. 21st Int. Conf. Chengdu, 2006) IAEA (2006).

0022-3115/$ - see front matter © 2009 Elsevier B.V. All rights reserved.
doi:10.1016/j.jnucmat.2009.01.219

[2]. This allows a greatly improved tomographic reconstruction of the radiation pattern on a timescale of the order of the typical duration of a Type I ELM cycle (~1 ms). In addition, the new system permits for the first time on JET an accurate analysis of the total energy radiated by any particular ELM, even in the case of smaller, higher frequency Type III ELMs.

3. Results and discussion

The gas fuelling has been varied in a series of repeated ELMy H-mode 3.0 MA discharges with strike points located on the lower vertical tiles of the MkII-HD divertor to produce Type I ELMs of different sizes ($\Delta W_{ELM}/W_{ped}$ increases with decreasing gas fuelling) in the ELM energy range $\Delta W_{ELM} = 0.2 \rightarrow 0.9$ MJ. Discharges without gas fuelling show large (giant) ELMs with $\Delta W_{ELM} \approx 0.9$ MJ. Such ELMs are often followed by a phase of Type III ELMs (so-called 'compound' phase) or even a brief return to L-mode confinement. The 'global energy balance' for these discharges (energy balance integrated over the entire discharge) reads: total injected energy E_{in} in the range 160–195 MJ, radiated energy E_{rad} in the range 70–90 MJ, $E_{rad}/E_{in} \approx 0.45$, and deposited energies onto inner and outer divertor targets of ≈25 MJ and ≈71 MJ, respectively. The largest ELMs deposit on average ~10% of ΔW_{ELM} on main wall surfaces [3]. Despite the large influence of the gas fuelling on the ELM behaviour, the global energy balance shows negligible variations with different gas levels and correspondingly with different ELM sizes.

Fig. 1 shows the divertor radiation distributions integrated over two different phases during a large ELM with $\Delta W_{ELM} \sim 0.9$ MJ. The first phase, of ~4 ms duration, includes radiation during the Type I ELM crash and the second (~14 ms) during the Type III ELMs phase (compound phase) which follows. The time intervals (phases I and II) delimit the time over which the bolometry signals have been averaged. In both phases the radiation distribution is strongly weighted to the inner divertor region (in–out asymmetries of ~*a* factor 3 in phase I). The in–out asymmetry is defined as the ratio of integrated radiation signals over inner and outer divertor legs. Both signals exclude the radiation around the X-point. This is also the case during the inter-ELM period, but with a lower asymmetry factor of ~2. This reflects the higher density, cooler plasma at the inboard divertor for forward toroidal field operation. The total radiated energy during the Type I ELM, evaluated by an algorithm similar to that described in [4], is 570 kJ, corresponding to 72% of the ELM energy losses ($\Delta W_{ELM} \approx 790$ kJ). It is important to note that the radiated power is determined by the radiation from the particle release due to the ELM-target interaction together with the changes in the local plasma parameters provoked by the ELM.

Along with the critical question of the radiated energy during the Type I phase, the radiated energy during the compound phase is an important parameter. A strong degradation of the plasma energy was observed during the compound phase; analysis of the radiation occurring during this phase shows that it accounts for a significant fraction (up to 90%) of the plasma energy loss.

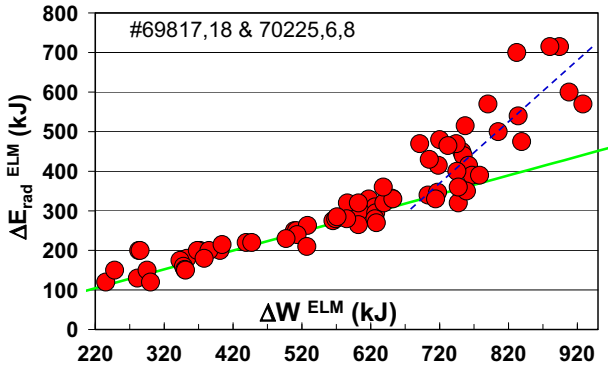

Fig. 2. Radiated plasma energy following Type I ELMs versus ELM energy loss.

Fig. 2 presents the dependence of the radiated plasma energy following the ELM crash on ΔW_{ELM}. Here the radiated energy contains only the part of the radiated losses which occurs during the first main peak during the ELM. For an ELM energy below 700 kJ (roughly), the radiated plasma energy is proportional to the ELM energy, as expected from the observed linear correlation between impurity influxes and ELM sizes. In this range the ELMs radiates ~50% of the ELM energy drop.

Beyond a ΔW_{ELM} of ~700 kJ, a non-linear increase of the divertor radiation occurs which is interpreted as an indication of additional carbon ejection from the target tiles, possibly due to material ablation. The target surface temperature during the transient loads as measured with infra-red thermography reaches peak values significantly below of ~2000 °C at the inner divertor. A detailed discussion about peak temperature values attained during the large ELMs is given in [3]. Even the maximum value of 2000 °C is too low for bulk carbon ablation which would correspond to a carbon sublimation of about 10^{19} C/m^2 s at this temperature, yielding a total release of 2×10^{19} C/s for a 0.5 m^2 loaded surface during the ELM. This quantity of carbon is much smaller than the known intrinsic carbon sources (~10^{21} C/s from the main wall and ~7×10^{21} C/s from the divertor [5]). The enhanced radiation losses over $\Delta W_{ELM} \sim 700$ kJ can be explained with high confidence by the ablation of the re-deposited carbon layer which is known to exist on the inner divertor target. The ablation of layer may be accompanied by the release of macroscopic clusters. The inner divertor is always a region of net deposition on JET and the outer of net erosion for standard forward field operation [6]. These

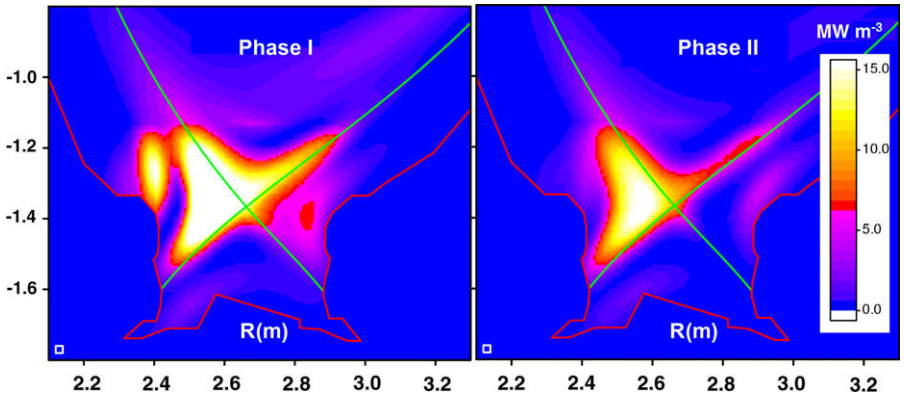

Fig. 1. Typical radiation distribution for large ELMs.

layers with poor thermal contact and low thermal capacity respond much more strongly to the power flux than the bulk target tiles. The re-deposited layers in the inner divertor contain a large amount of Be (up to 50%). Interestingly, the fast signals in BeII- and CIII-emission react at the same time (~300 μs after fall in plasma energy) during the transient events, confirming the assumption of ablation of deposited layers in the inner divertor. This results are consistent with previous spectroscopic measurements [7] indicating the strong C_2 and CD emission in ELMing H-mode discharges with strike points positioned on the horizontal divertor tiles where soft a-C:H layers are formed by redeposition of carbon eroded from the vertical tiles.

As mentioned above, the inter-ELM radiation distribution is always strongly weighted to the inner divertor volume (in–out asymmetries of ~factor 2). The ELM exacerbates this radiation asymmetry, with the magnitude of the increase linearly dependent on the ELM energy in the range $\Delta W_{ELM} \sim 100$–600 kJ (see Fig. 3). This indicates that the deposited layers play a key role, especially since peak temperatures at the outer target are even higher than those observed on the inner side [3]. It is assumed that the impurity release is a likely combination of a thermal decomposition of the layer and of ablation. For $\Delta W_{ELM} > 600$ kJ the in–out asymmetry shows a 'break' in the linear dependence. One explanation for this observation is the hypothesis that ablated material can reach the outer divertor via the private flux region and thus contribute to the radiation in the outer divertor volume. Secondary peaks on fast CIII divertor spectroscopy with ~0.5 ms delay compared with the first peak at the outer divertor confirm this assumption. This time delay is approximately equal to the divertor transit time for thermal carbon atoms and C_2 molecules. Such a process is also assumed in [8] as an explanation of the non-linear increase in the erosion measured in JET beyond a given ELM size using Quartz Micro Balance detectors. Additionally, Fig. 3 (right) shows the radiation distribution for ELMs with medium and large sizes. For large ELMs the radiation 'spills over' into the outboard X-point region.

The impurity influxes associated with transient events can have a significant influence on the discharge since they can lead to an increased plasma contamination and even to a radiative collapse. Fig. 4 shows the radiation profiles for ELMs with large sizes. This analysis shows a strong increase of the radiation in the edge (normalised minor radius $\rho > 0.8$) during the largest events in the database. The profile during the 'compound' phase clearly shows increased radiation in the plasma core and correspondingly points to an increased plasma contamination. An increase of Z_{eff} by about $\Delta Z_{eff} \approx 0.4$–0.5 has been observed in the compound phase.

Other important events which are dangerous for plasma-facing components are the power loads onto the wall during disruptions, MARFEs and VDEs. The energy loss in disruptions can be divided into two phases as shown in Fig. 5: first the thermal energy is lost to the walls in the thermal quench. This is then followed by the loss of the energy stored in the poloidal magnetic field in the current

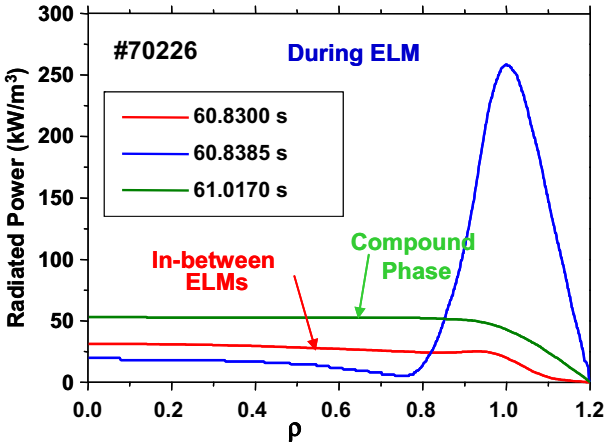

Fig. 4. Radiative profiles for ELMs with large sizes.

quench. The current quench occurs because the plasma becomes extremely resistive when its temperature drops in the thermal quench. This implies a large Ohmic heating power in which the energy stored in the plasma magnetic field is dissipated as thermal energy in the plasma. While the temperature is low, the plasma is also extremely radiative. The energy balance studies of the JET disruptions [9] have indicated that the magnetic energy transferred to the plasma by Ohmic heating in the current quench is mostly radiated to the first wall.

The tomographic reconstruction model which is used (anisotropic diffusion model) has been coupled with a Monte-Carlo technique to calculate the poloidal radiation distribution, hence the radiation load onto the vessel, during these transient events. The radiation distribution is strongly poloidally asymmetric in particular in the current quench as shown in Fig. 5. Fig. 6(b) shows the evaluated radiation peaking factors (the local radiation power load onto the wall normalised to its value averaged over the entire surface) as function of the poloidal distance along the wall (Fig. 6(a)) for two types of disruptions (density limit disruption already discussed in Fig. 5 and disruption driven by Neoclassical Tearing Mode). A maximum of the observed radiation peaking factor for the disruption current quench of about 2.5 is observed. It is located at the inner main chamber wall. A maximum of the observed radiation peaking factor for MARFEs is of about 4.5, and below 5 during VDEs. The radiation peaking occurs at the outer divertor target during the X-point MARFE. These 'peaking factors' have been used to extrapolate to ITER reference conditions. With the poloidal magnetic energy of ITER of ~600 MJ and a current quench time of ~36 ms [10], a maximum radiative load of 61 MW/m^2 is obtained assuming a radiation peaking factor of 2.5. This type of radiation losses (for the current quench alone) may increase the Be temperature to about half the melting point.

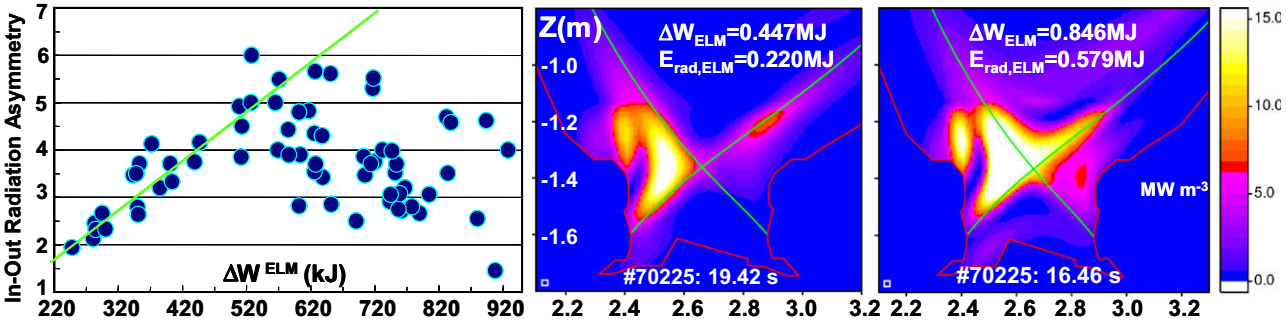

Fig. 3. In–out radiation asymmetry versus ELM energy loss and radiation reconstructions for medium and high ΔW_{ELM}.

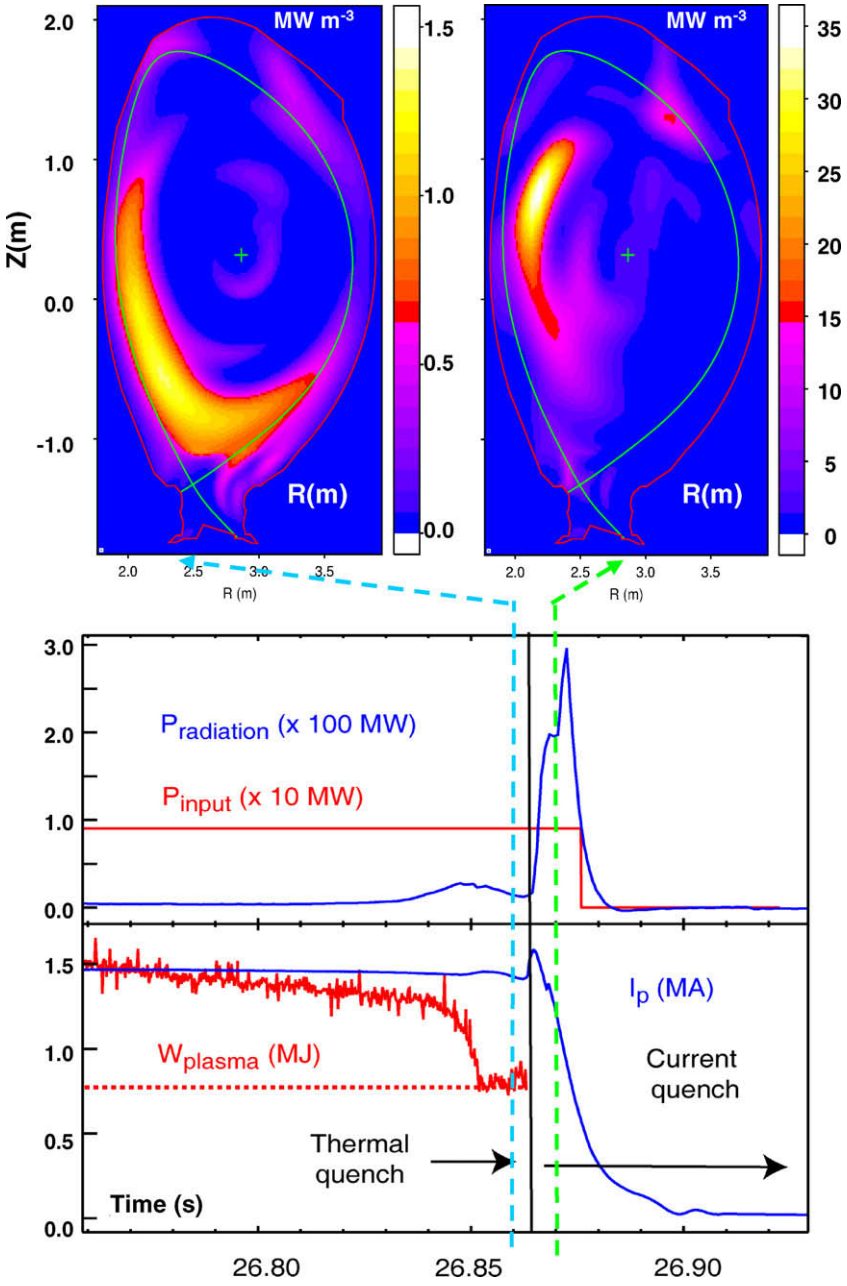

Fig. 5. Radiation distribution during the disruption.

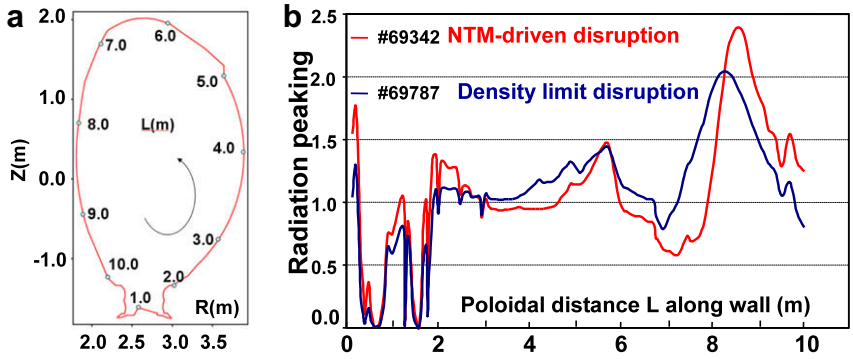

Fig. 6. Radiation peaking factors during the current quench in JET.

4. Summary and conclusion

ELM radiation behaviour has been analysed in detail in the Type I ELMy H-mode regime, which is the baseline scenario for operation of ITER at high fusion gain. A significant part of the total ELM energy loss can be found in form of plasma radiation, located mostly in the divertor region. The total radiation amounts to about 50% of the ELM losses for ELMs between 0.1 MJ and 0.9 MJ. The ELM-induced radiation is always higher at the inner than at the outer divertor with an approximately linear increase of the asymmetry up to a total ΔW_{ELM} of about 0.6 MJ and a decrease for higher ΔW_{ELM}. Large Type I ELMs with energy losses above 0.65–0.7 MJ show enhanced radiation losses which are associated with the ablation of carbon layers in the inner divertor, a result corroborated by the spectroscopic measurements on beryllium. Analysis of compound ELMs (Type I ELM followed by a phase of Type III ELMs) shows that radiated energies during the Type I ELM are in the range of 15–50% of ΔW_{ELM}. A significant fraction (up to 90%) of the plasma energy degradation observed during the compound phase is found in the form of plasma radiation. The radiation profile during the 'compound' phase clearly shows increased radiation in the plasma core and correspondingly points to an increased plasma contamination.

It is found that the radiation distribution during the transient events is poloidally asymmetric with a maximum of the observed 'radiation peaking factor' (RPF) for the disruptive current quench of 2.5 and for MARFEs of about 4.5, and less than 5 during VDEs. These RPFs have been used to extrapolate to ITER reference conditions. The radiation loss during the disruptive current quench alone (RPF = 2.5) will increase the beryllium temperature to about half the melting point.

Acknowledgement

This work, supported by the European Communities under the contract of Association between EURATOM and FZJ, was carried out within the framework of the European Fusion Development Agreement. The views and opinions expressed herein do not necessarily reflect those of the European Commission.

References

[1] ITER Physics Basis Editors, Nucl. Fus. 39 (1999) 2137.
[2] A. Huber, K. McCormick, P. Andrew, et al., Fus. Eng. Des. 82 (2007) 1327.
[3] R.A. Pitts et al., J. Nucl. Mater. 390–391 (2009) 755.
[4] J.C. Fuchs, T. Eich, A. Hermann, et al., J. Nucl. Mater. 337–339 (2005) 756.
[5] J.D. Strachan, W. Fundamenski, M. Charlet, et al., Nucl. Fus. 43 (2003) 922.
[6] J.P. Coad et al., Nucl. Fus. 46 (2006) 350.
[7] S. Brezinsek et al., J. Nucl. Mater. 337–339 (2005) 1058.
[8] A. Kreter et al., J. Nucl. Mater. 390–391 (2009) 38.
[9] J.I. Paley et al., J. Nucl. Mater. 337–339 (2005) 702.
[10] J.C. Wesley et al., 2006 IAEA Fusion Energy Conference (Chengdu, China), Paper IT/P1-21.